POLITECNICO DI TORINO
Repository ISTITUZIONALE

Translating node of Ranvier currents to extraneural electrical fields: a flexible FEM modeling approach

(Article begins on next page)

25 April 2024

Translating node of Ranvier currents to extraneural electrical fields: a flexible FEM modeling approach

Fabiana Del Bono[1,2], Adrien Rapeaux[2,3], Danilo Demarchi[1] and Timothy G. Constandinou[2,3]

Abstract— Simulations of electroneurogram recording could help find the optimal set of electrodes and algorithms for selective neural recording. However, no flexible methods are established for selective neural recording as for neural stimulation. This paper proposes a method to couple a compartmental and a FEM nerve model, implemented in NEURON and COMSOL, respectively, to translate Node of Ranvier currents into extraneural electric fields. The study simulate *ex-vivo* experimental conditions, and the method allows flexibility in electrode geometries and nerve topologies. This model has been made available in a public repository[4]. So far, the model behavior complies with available experimental results and expectations from literature. There is good agreement in terms of signal amplitude and waveform, and computational times are acceptable, leaving room for flexible simulation studies complementary to animal tests.

I. INTRODUCTION

Electrodes for peripheral nerve interfaces come in different degrees of invasiveness, that is directly related to selectivity [1]. Cuff electrodes have been proven to be stable *in-vivo* for over 10 years in the body, therefore they are the most suitable for chronic applications [2]. However, they show a poor degree of selectivity. If used for recording, they sense electrical potentials at the level of the epineurium, and cannot resolve the underlying sources that generated the signal. To achieve recording selectivity, multiple contacts are used in different configurations. Multielectrode cuffs (MECs) feature several metallic rings allowing several recording channels in the longitudinal direction, while in Multicontact cuffs the rings are further split into several contacts along the circumference. To extract information, algorithms have been developed in addition to traditional signal processing to achieve selective recording: velocity selective recording for MECs [3], source localisation [4] and matched filters [5] for MCCs. Selective recording studies are usually conducted *ex-vivo* [6], [7] or *in-vivo* [8], [9] by mechanically or electrically stimulating the receptors or the nerve, respectively [10]. Finding an optimal setup is not trivial, as testing different electrode configurations is burdensome on

[1]Fabiana Del Bono and Danilo Demarchi are with the Department of Electronics and Telecommunications, Politecnico di Torino, 10129 Torino (TO), Italy `fabiana.delbono@polito.it`, `danilo.demarchi@polito.it`

[2]Adrien Rapeaux and Timothy Constandinou are with the Department of Electrical and Electronic Engineering, Imperial College London, South Kensington Campus, London, SW7 2AZ, UK. `adrien.rapeaux13`, `t.constandinou@imperial.ac.uk`

[3]Adrien Rapeaux and Timothy Constandinou are also with the Care Research & Technology Centre, UK Dementia Research Institute, UK.

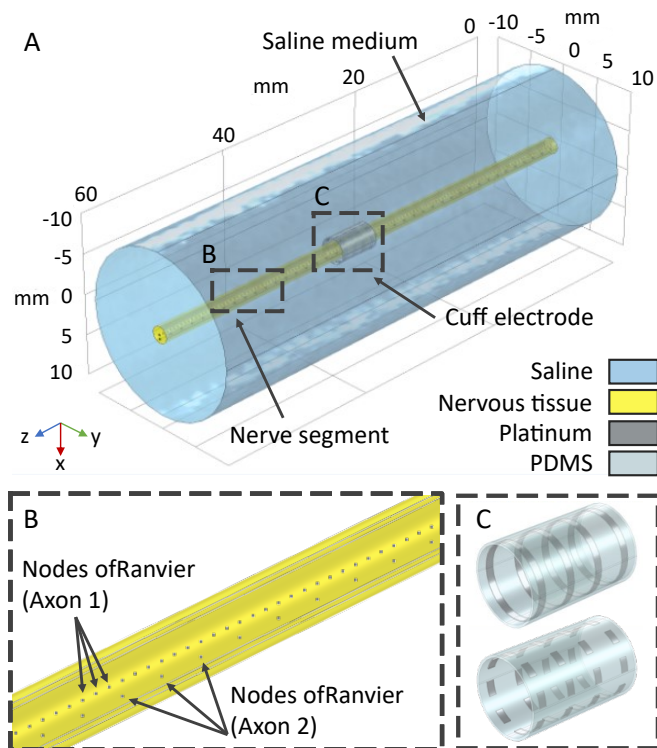[4]https://github.com/fabianadelbono/PNrec

Fig. 1. Comsol model: (a) the nerve is modeled as a cylinder, enclosed in a cylinder of saline. Axons (b) are modeled as sequences of equally spaced points, the Nodes of Ranvier (NORs). The cuff electrode (c) in either MEC or MCC configuration, is placed in the middle of the length. Point current sources are assigned to the NORs, Ground is assigned to the external cylinder, its bases are defined as electrical insulation.

time and resources. Although potentially enabling a cost-effective study of selective recording methods, simulations of recordings from peripheral nerves are not as widespread among researchers as their counterparts for stimulation, for which the majority of existing setups has been developed [7]. Approaches span from axon-level [11], [12], [13] to whole nerve simulations [14], [15], [16], each focusing on a different level of the fascicular structure of the nerve.

For recording simulations, models that feature the most detailed topology [17] are commercial software Sim4life (Zurich MedTech AG), PyPNS [18] and the work of Zariffa et al [19]. They include anisotropic FEMs that model the 3D structure of the nerve. However, even though very flexible in the representation of the nerve composition, [18] features precomputed electric fields and doesn't allow testing different recording electrode geometries. The work described in [19] instead uses a very detailed model of the nerve
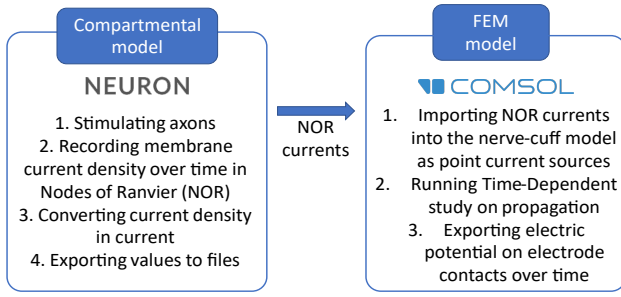
Fig. 2. Overview of the workflow. Data, consisting of the currents in the nodes of Ranvier (NORs), flows unidirectionally from Neuron to Comsol.

tissues, but lacks variety in terms of the fibres composing the bundle. In this study we provide for the first time an effective workflow able to guarantee both flexibility in the definition of the nerve and electrode structures and reliability of the results, with a potential use for developing and testing the widest range of selective recording algorithms. To the best of the authors' knowledge, an accessible platform that allows the simulation of non-invasive recording of neural activity with fine control over electrode properties and signal sources doesn't exist. The work presented here aims to bridge this gap by creating a method that synergically interfaces widespread software such as NEURON and COMSOL. The premise is translating the currents in each node of Ranvier (NOR) obtained with compartmental models into current sources in FEM using a quick and repeatable workflow (Fig. 2) with a computationally effective process. The following sections in the paper will detail the use of the tools within the process and the results obtained, together with a discussion on their reliability, the margins for improvement and future perspectives.

II. MATERIALS AND METHODS

The simulated setup replicates an *ex-vivo* experiment, where a 6 cm long and 1-2 mm diameter nerve is coupled with a cuff electrode placed at its midpoint. The nerve is electrically stimulated at one extremity and the resulting potentials are recorded.

The method incorporates FEM modeling to allow for flexibility in defining nerve topology. The workflow reverses what is generally implemented in computational studies of stimulation [14], exploiting a unidirectional coupling between NEURON and COMSOL. Instead of generating fields in FEM and applying them to a compartmental model, data from the compartmental model is now imported into COMSOL. This leads to some issues in managing the amount of information to be exchanged in the software. Membrane dynamics of the axons are simulated within NEURON, and its output in membrane current on each NOR is translated in point current sources within COMSOL. Finally, a time-dependant study is run to visualise action potential (AP) propagation in the nerve and predict recorded extraneural potentials at specific cuff contact locations.

A. Compartmental model

Compartmental models are the most popular approach for simulating electrophysiology in neurons. They have been used both at fibre scale [20], [13], [11] and for inclusion into FEM models for nerve stimulation [15], [16]. This model has been used for simulating the generation of APs within the single axons composing a nerve.

Although the mathematical abstraction underlying a compartmental model makes it implementable in a wide range of software packages and even embeddable into FEM [16], the NEURON simulation environment [21] has been preferred for its flexible approach, allowing the user to focus on the neurophysiology. Models already available in NEURON such as the mammalian nerve fibre named the MRG axon [11] have been validated experimentally. Due to its reliability, it has been included in several simulation studies, in particular for stimulation [22], [14], and in the above mentioned PyPNS [18]. The model, available at [23] has been customised to fit the needs of this study. The final parameters used are reported in table I.

The number of Nodes of Ranvier (NORs) has been changed from a fixed value to be dependent on the total length of the nerve l_{TOT}, defined as 60 mm, according to

$$n_{NOR} = \frac{l_{TOT}}{\Delta_x} \tag{1}$$

rounded to the smallest integer, where Δ_x is the spacing between the NORs. The current source for intracellular stimulation has been moved from the central NOR to the first NOR, and provides a stimulation pulse of 5 nA in amplitude and 0.1 ms in duration, with an onset time of 1 ms. The duration of a single simulation has been kept to 150 ms and the dt is 5 μs, leading to less than one minute simulation time with an Intel Core i7 8th Gen. processor. For each NOR segment, the corresponding membrane current density I_{mem} is extracted. The underlying assumption is that just the NORs contribute to the extraneural potentials recorded by the cuff, given the insulating effect of the myelin sheath. To make the values compliant with the definition of point current sources in COMSOL, the latter is converted into a total current

$$I_{PCS} = I_{mem} * S_{NOR} = I_{mem} * \pi d_{axon} l_{NOR} \tag{2}$$

where I_{PCS} is the current for the equivalent point current source, I_{mem} is the membrane current density, S_{NOR} is the NOR surface, that takes into account the axon diameter d_{axon} and the NOR length l_{NOR} (fixed to 1 μm).

TABLE I
ELECTRICAL PARAMETERS IN NEURON SIMULATION

Specific nodal capacitance	2 μF/cm^2
Axoplasmic resistivity	70 Ω*cm
Periaxonal resistivity	70 Ω*cm
Extracellular resistivity	500 Ω*cm
Maximum nodal fast Na+ conductancee	3 S/cm^2
Maximum nodal slow K+ conductance	0.08 S/cm^2
Maximum nodal persistent Na+ conductance	0.005 S/cm^2
Maximum nodal leakage conductance	0.08 S/cm^2

The MRG axon model provides parameters for simulating 9 different nerve diameters. Given the limited amount of fibres imported so far in the FEM Model, this study didn't require the expansion of these with additional diameters. The currents from the NORs are automatically exported to formatted *.txt* files, suitable to be imported as a table in COMSOL.

B. FEM model

The FEM model has been developed in COMSOL Multiphysics, being a flexible and well established simulation environment in engineering. In all its steps, this study benefited from the use of Java programming tools provided by the *Application Builder*, which had a crucial role in automating repetitive tasks (e.g. creating geometries, importing current data, exporting results). Given the high amount of geometric entities to be created and functions to be imported or exported, setting up the model manually would have made the process exponentially more time consuming and compromised the flexibility of the platform. On the contrary, automating tasks enables the user to define the simulation parameters, running functions to have the model set up automatically. The proposed model is presented in Fig. 1.

The nerve is modeled as a cylindrical structure, enclosed in a 20 mm diameter cylinder of 0.9% NaCl saline solution. Within the nerve, each axon is represented as a sequence of NORs, defined as points equally spaced according to their definition in NEURON and parallel to the nerve central axis. In this phase of the study, to reduce computational time in the absence of a high-power computing cluster, the whole nerve tissue has been represented according to the values reported in [24] at the frequency of 3 kHz (power peak of electroneurograms). The properties set for the simplified materials are reported in table II.

TABLE II
MATERIAL PROPERTIES IN FEM MODEL

	Electrical conductivity (S/m)	Rel. permittivity
Saline	1.45	1
Nerve tissue	0.03	70000
PDMS	2.5e-14	2.75
Platinum	8.9e6	0.7

Cuff electrodes are modeled separately and their geometries imported into the model. Two templates were created, MEC and MCC, neglecting the closing mechanism and sutures or wires and representing the structure as a PDMS tube with platinum contacts. Templates are parameterised so that the geometry can be modified from the parameters section according to the user's needs, in terms of cuff length, diameter, thickness, and contact number and spacing.

The problem has been studied by applying *Electric Currents* physics to the entire domain, as included in the *AC/DC* module. NORs were modeled as point current sources, where current output was informed by NEURON. Currents from subsequent points in Neuron give a similar waveform (see the AP, Fig. 3a), delayed over time as soon as the potential propagates along the fibre. The outer cylinder of saline has its potential set to *Ground*, its bases marked as *Electrical insulation*.

The simulation has been configured as a *time-dependent study*, so as to evaluate the effect of the AP propagation both from one NOR to another and from the NORs to the electrodes through the bulk. The observation window has been set between 1 and 4 ms, an interval in which the potentials on all the NORs appear and fade away, with a time step of 10 µs i.e. double that of the NEURON simulation, to reduce computation time. To avoid errors due to approximations, the solver has been set with a variable scaling of 10^{-4}, which was found as an optimal value.

The simulation results are visualised as heatmaps of the electric potential in Volume and Slice plots (Fig. 3b), so as to show the propagation of the APs. Additionally and more importantly, volume averages of the electric potential on each electrode contact are created, giving the recording of the signal over time, and exported as .txt files to be processed in a numeric computing environment (e.g. Matlab). An example of a plot is shown in Fig. 3c.

III. RESULTS

The system was tuned by assessing the effect of the basic parameters in geometry, materials, physics, mesh and study configuration to optimise computational efficiency, resulting in computation time between 5 and 15 minutes. Waveforms obtained at this step showed monopolar recording amplitudes of approximately 1 µV. This was compared with experimental data collected by researchers at Imperial College London where CAP amplitudes are reported to be between 0.8 and 1.2 mV. As this takes into account contributions from many fibres firing at the same time in the nerve, simulated peak to peak values were multiplied by the average number of myelinated fibres in the rat sciatic nerve [25], obtaining an estimated CAP amplitude in the range of 0.8 to 30 mV. A comparison of the waveforms for simulated and experimentally recorded A-fibre CAP in bipolar recording conditions is provided Fig. 4.

Following these tests, the behaviour of the signal according to the changes in the cuff electrode geometry was investigated. Given the simulation parameters provided in table III, two series of simulations were performed.

TABLE III
STATIC SIMULATION PARAMETERS

Nerve-saline length	60 mm
Nerve diameter	2 mm
Saline diameter	20 mm
Cuff thickness	100 µm
Cuff length	5 mm
Cuff diameter	3 mm
Cuff rings	4
Cuff contacts/ring (MCC model)	8
Contact width	300 µm
Longitudinal IED	1.333 mm
Mesh setting	'Finer'
Fibre type (single fibre model)	16 µm MRG

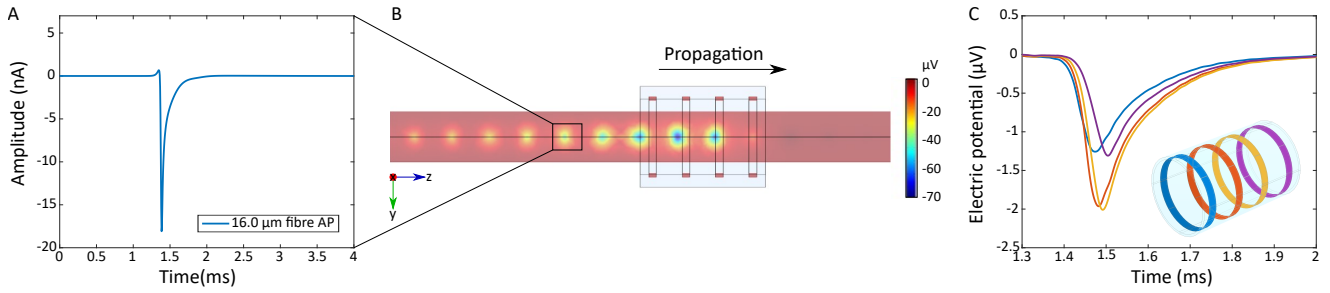First, cuff length was swept from 5 to 8 mm with step size of 0.5 mm, keeping inter-electrode distance constant, to

Fig. 3. Example of a simulation in a 16 μm diameter central fiber. The current outputs from NEURON simulation (a) determine the action potentials inside the nerve, with a delay between consecutive nodes due to the saltatory conduction simulated in the compartmental model. Propagation is highlighted in (b), where the central portion of the nerve is represented, and sensed by an MEC electrode). The recorded potentials are represented in (c). The delay between waveforms can be seen, containing longitudinal information, together with the difference in amplitude between the outermost contacts, closer to the edges and less affected by the insulating effect of the cuff.

test the effect of incrementing the distance from the outer electrode rings to the edge of the insulating tube. Second, diameter was swept from 2 to 3.5 mm with variable step size, to test the influence of the saline medium between nerve and cuff on the amplitude of the recorded potentials. Results of these two sets of simulations are shown in Fig. 5.

In the last stage, an MCC with 32 contacts distributed on 4 rings was tested on varying nerve topologies with 1, 2 or 9 fibres at variable locations in the nerve cross-section. Recordings from each contact were visualised to highlight the differences in recorded waveforms according to the position of each contact with respect to the nerve length and fibre position. An example of output from this test is shown in Fig. 6, obtained with a topology featuring 9-fibres.

IV. DISCUSSION

The model showed results in good agreement with experimental conditions, taking into account the approximations that have been introduced. The overestimation of the computed CAP amplitude with respect to the experimentally recorded ones can be explained in two ways. First, nerve bundle anisotropies and perineurium resistivity [15] aren't modeled. Their introduction into the FEM model will substantially lower the peak-to-peak amplitude of the recorded APs. Second, CAP amplitude estimation does not account for

differences in conduction velocities within a nerve population, nor for differences in electric fields generated by larger and smaller fibres.

The surface and slice plots correctly show the propagation of the APs from one NOR to another over time (Fig. 3b), with different conduction velocities according to fibre size. Recordings on subsequent rings show a delay in the recorded peaks associated with propagation. Signal amplitudes for outer rings are lower as shown Fig. 3c. The latter effect can be explained by the insulating effect of the cuff, that is less pronounced near its edges. This is supported by testing varying cuff lengths (Fig. 5a), where amplitude increases linearly with contact distance from the edge. The role of insulation is also evidenced in the diameter test (Fig. 5b), where a 10% diameter increase approximately halves the recorded signal amplitude. This aspect is crucial in experimental conditions, especially *in-vivo*, where the cuff serves to increase the SNR both by constraining electric fields generated by APs and shielding the electrodes from external noise sources. However, cuffs should avoid mechanically constraining the nerve, leading to a trade off on cuff dimensions. Additionally, tests with multiple fibres suggest the model is a promising tool for developing and testing selective recording algorithms. As Fig. 6 shows, monopolar recordings of a CAP produced by 9 fibres differ from the first and last ring, showing separation of
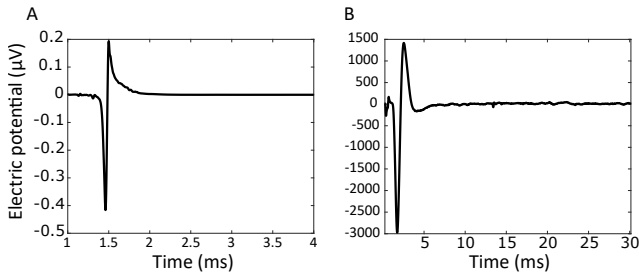

Fig. 4. (a) Simulated bipolar recording from single fibre, compared with (b) a potential recorded experimentally from A fibres in a rat sciatic nerve. Discrepancies in amplitude are compatible with fibre count in rat sciatic nerves [25]. The longer time period on the real recording (b) can be explained by differences in firing times and ion channel dynamics from one fibre to the other, causing the signal to spread out over time.
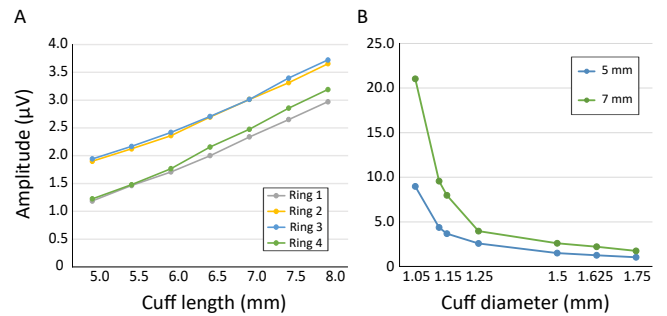

Fig. 5. Results of the tests on cuff geometrical parameters, on a nerve with a 16 μm diameter central fibre. The effect of cuff length (a) and cuff diameter (b) are shown, showing a linear and an inverse dependence, respectively, on the values in the simulated range, and pointing out the dependence of the signal quality on the insulating effect of PDMS.
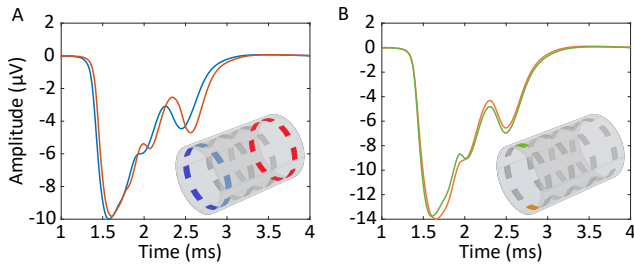
Fig. 6. Monopolar MCC recording of CAPs produced in a 9-fibers nerve model. In (a), the difference in propagation velocity of the fibres is evidenced by the spreading of the peaks of the single APs, while in (b) the morphological differences on opposing contacts along nerve circumference are shown. This information is exploitable by selective recording algorithms.

the AP as long as the signal propagates along the nerve, but also from opposing rings, with differences in the amplitude of the relative peaks corresponding to different fibres. This proves that spatial information is also contained in the simulated MCC recordings and the model can serve not only as a surrogate for *ex-vivo* tests, but also in a complementary role. For example, machine learning techniques could benefit from the knowledge of signal source positions and timings.

V. CONCLUSION

This study provided a method for simulating the potentials produced by NOR currents within the nerve in a FEM model and recording them with a cuff electrode, with the novelty of a workflow that allows extreme flexibility in the definition of electrode geometries and nerve composition and topology. The model is a tool that is usable besides or as a surrogate of *ex-vivo* tests, with the advantages of a simulation study. The main ones are the test of any kind of cuff electrode design under a variety of conditions, with consequent resource optimisation, as well as control over signal sources within the nerve with a detail that is impossible to replicate in lab tests. Thanks to the latter, it can potentially push forward the study, design and development of signal processing and classification algorithms for selective recording in peripheral nerves. The model is open and ready for improvement, in particular for increasing the number of fibres, supported by the development of new fibre models within neuron by extrapolation of the existing parameters, the definition of more complex and realistic materials, the modeling of the membranes and anisotropies, the test of other electrode models, such as intraneural, and the simulation of spontaneous activity. Simulation times up to now have been quite short with a maximum of 15 minutes, however adding complexity to the model may make running them on single computer impractical, at which point a High Power Computing cluster should be considered.

ACKNOWLEDGEMENT

REFERENCES

[1] C. E. Larson and E. Meng, "A review for the peripheral nerve interface designer," *J. Neurosci. Meth.*, vol. 332, no. June 2019, p. 108523, 2020. [Online]. Available: https://doi.org/10.1016/j.jneumeth.2019.108523

[2] B. P. Christie et al, ""Long-term stability of stimulating spiral nerve cuff electrodes on human peripheral nerves"," *Journal of NeuroEngineering and Rehabilitation*, vol. 14, no. 1, pp. 1–12, 2017.

[3] J. Taylor et al, "A summary of current and new methods in velocity selective recording (VSR) of electroneurogram (ENG)," *Proc. IEEE ISVLSI*, vol. 07-10-July-2015, no. July 2015, pp. 221–226, 2015.

[4] J. Zariffa and M. R. Popovic, "Application of EEG source localization algorithms to the monitoring of active pathways in peripheral nerves," in *Proc. IEEE EMBC*, 2008, pp. 4216–4219.

[5] R. G. Koh, A. I. Nachman, and J. Zariffa, "Classification of naturally evoked compound action potentials in peripheral nerve spatiotemporal recordings," *Scientific reports*, vol. 9, no. 1, p. 11145, 2019.

[6] H. Kim et al, "Cuff and sieve electrode (case): The combination of neural electrodes for bi-directional peripheral nerve interfacing," *J. Neurosci. Meth.*, vol. 336, p. 108602, 2020.

[7] A. Rapeaux and T. G. Constandinou, "An HFAC block-capable and module-extendable 4-channel stimulator for acute neurophysiology," *J. Neural Eng.*, vol. 17, no. 4, p. 046013, 2020.

[8] P. B. Yoo and D. M. Durand, "Selective recording of the canine hypoglossal nerve using a multicontact flat interface nerve electrode," *IEEE Trans. Biomed. Eng.*, vol. 52, no. 8, pp. 1461–1469, 2005.

[9] A. Rapeaux, E. Brunton, K. Nazarpour, and T. G. Constandinou, "Preliminary study of time to recovery of rat sciatic nerve from high frequency alternating current nerve block," in *Proc. IEEE EMBC*, 2018, pp. 2671–2674.

[10] S. Luan, I. Williams, K. Nikolic, and T. G. Constandinou, "Neuromodulation: present and emerging methods," *Frontiers in neuroengineering*, vol. 7, p. 27, 2014.

[11] C. C. McIntyre et al, "Modeling the excitability of mammalian nerve fibers: Influence of afterpotentials on the recovery cycle," *J. Neurophysiology*, vol. 87, no. 2, pp. 995–1006, 2002.

[12] H. Parasuram et al, "Computational modeling of single neuron extracellular electric potentials and network local field potentials using LFPsim," *Front. Comput. Neurosci.*, vol. 10, no. Jun, pp. 1–13, 2016.

[13] W. M. Grill, "Modeling the effects of electric fields on nerve fibers: Influence of tissue electrical properties," *IEEE Trans. on Biomedical Engineering*, vol. 46, no. 8, pp. 918–928, 1999.

[14] A. Rapeaux, K. Nikolic, I. Williams, A. Eftekhar, and T. G. Constandinou, "Fiber size-selective stimulation using action potential filtering for a peripheral nerve interface: A simulation study," *Proc. IEEE EMBC*, vol. 2015-Novem, pp. 3411–3414, 2015.

[15] N. A. Pelot, C. E. Behrend, and W. M. Grill, "On the parameters used in finite element modeling of compound peripheral nerves," *J. Neural Eng.*, vol. 16, no. 1, 2019.

[16] I. Tarotin, K. Aristovich, and D. Holder, "Simulation of impedance changes with a FEM model of a myelinated nerve fibre," *Journal of Neural Engineering*, vol. 16, no. 5, p. 056026, sep 2019. [Online]. Available: https://doi.org/10.1088/1741-2552/ab2d1c

[17] T. Hayami, K. Iramina, and X. Chen, "Computer simulation of nerve conduction study of a sural nerve to evaluate human peripheral nervous system," *IFMBE Proceedings*, vol. 63, pp. 461–465, 2018.

[18] C. H. Lubba et al, "PyPNS: Multiscale Simulation of a Peripheral Nerve in Python," *Neuroinformatics*, vol. 17, no. 4, p. 629, 2019.

[19] J. Zariffa and M. R. Popovic, "Localization of active pathways in peripheral nerves: A simulation study," *IEEE Trans. on Neural Systems and Rehabilitation Engineering*, vol. 17, no. 1, pp. 53–62, 2009.

[20] J. D. Sweeney, J. T. Mortimer, and D. Durand, "Modeling of Mammalian Myelinated Nerve for Functional Neuromuscular Stimulation." *Proc. IEEE EMBC*, no. January 1987, pp. 1577–1578, 1987.

[21] M. L. Hines and N. T. Carnevale, "The NEURON Simulation Environment," *Neural Computation*, vol. 9, no. 6, pp. 1179–1209, 1997.

[22] N. A. Pelot, B. J. Thio, and W. M. Grill, "Modeling current sources for neural stimulation in COMSOL," *Front. in Computational Neurosci.*, vol. 12, no. June, pp. 1–14, 2018.

[23] C. C. McIntyre. "ModelDB: Spinal Motor Neuron". [Online]. Available: https://senselab.med.yale.edu/modeldb/ShowModel?model=3810

[24] IT'IS Foundation. "Tissue Frequency Chart by IT'IS Foundation". [Online]. Available: https://itis.swiss/virtual-population/tissue-properties/database/tissue-frequency-chart/

[25] H. Schmalbruch, "Fiber composition of the rat sciatic nerve," *The Anatomical Record*, vol. 215, no. 1, pp. 71–81, 1986.